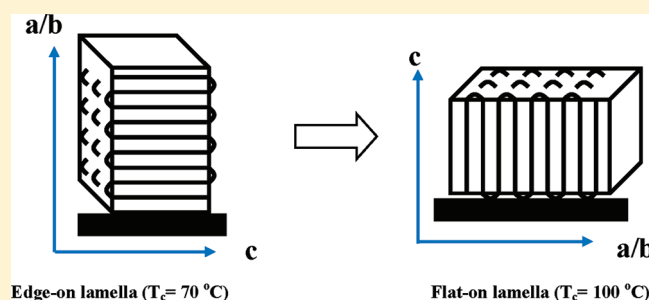


# Lamellar Orientation and Crystallization Dynamics of Poly (L-Lactic Acid) Thin Films Investigated by In-Situ Reflection Absorption Infrared Spectroscopy

Ningjing Wu, Meichun Ding, Chenwei Li, Yuan Yuan, and Jianming Zhang\*

Key Laboratory of Rubber-Plastics, Ministry of Education/Shandong Provincial Key Laboratory of Rubber-plastics, Qingdao University of Science & Technology, Qingdao City 266042, People's Republic of China

**ABSTRACT:** In situ reflection–absorption infrared (RAIR) spectroscopy was used to investigate the molecular orientation and crystallization dynamics of PLLA thin films crystallized at various temperatures. The results show that the annealing temperature has significant effect on the lamellar orientation of PLLA thin films, which is confirmed by atomic force microscopy (AFM) data. It is found that edge-on lamellar crystals of PLLA thin films are mainly formed by cold crystallization at low temperatures (70–90 °C), whereas the flat-on crystals occur when the crystallization temperature reaches to 100 °C. Of particular note, our in situ RAIR data collected during the whole isothermal crystallization process suggests that the orientation of PLLA chain takes place in the early stage of the crystallization process. Moreover, the analysis on the crystallization dynamics of PLLA thin film indicates that the crystal growth dimensional and nucleation modes are also strongly affected by the crystallization temperature.



## 1. INTRODUCTION

It is well-known that the structure and physical properties of polymer thin films are significantly different from those of their bulk sample.<sup>1–4</sup> For example, many reports have shown that the glass transitions of amorphous polymer thin film are changed greatly with decreasing the thickness less than 100 nm.<sup>4</sup> As for semicrystalline polymer, the complex self-assembling morphologies and dynamics behaviors driven by chain crystallization in thin film also lead to diversity observations.<sup>5–12</sup> Undoubtedly, it is of great importance to understand the structural origin and physical principle underlying these unusual phenomena of polymer thin film.

Poly(L-lactic acid) (PLLA) is a biodegradable and biocompatible thermoplastic semicrystalline polymer. Meanwhile, it has comparable thermal and mechanical properties comparable to those of commercial polymers. Therefore, as one of the most popular bioplastics, PLLA has attracted significant interest in the past decade.<sup>13–26</sup> So far, the crystallization behavior and crystalline structure of PLLA bulk have been extensively studied by various techniques. It was found that the crystallization temperature has significant effect on the crystal modifications of PLLA.<sup>13–15,18,24–26</sup> That is, ordered  $\alpha$  form and disordered  $\alpha'$  can be formed at temperature above 120 and below 100 °C, respectively.<sup>14,15,26</sup> However, it is found that few studies have been carried out on the crystallization behavior of PLLA thin film.<sup>27–29</sup> Recently, Maillard et al.<sup>27</sup> studied the crystallization behavior of PLLA thin film (15 nm) at high temperature range between 125 and 160 °C by using in situ atomic force microscopy and they found that edge-on lamellae with a curvature, which is related to polymer chirality, were observed. In most cases, the

static morphologies and structures of polymer thin films have often been ex situ studied by AFM, TEM and SAXS/WAXD techniques. But it should be pointed out these techniques are usually hard to follow the dynamic structural changes in the polymer thin film on the molecular level.

As a complementary technique, IR spectra are sensitive to the local environment of molecular groups or chain segments. Thus, based on the solid band assignments, it can be actually used to probe the physical structures of polymer chains in various phases. For measuring the polymer thin film, p-polarized IR light with grazing incidence angle is required so that the information on the chain orientation and conformation can be detected at the same time.<sup>30–38</sup> Such technique is also named as reflection absorption infrared spectroscopy (RAIR).

In this paper, we used the in situ RAIR technique to investigate the structural evolution and molecular dynamics in PLLA thin film. By a homemade heating stage, the isothermal crystallization processes of PLLA thin film at various temperatures could be in situ monitored immediately after the sample was transferred to a heating stage with the preset temperature, which can avoid the effect caused during the heating process. Our results show that various orientation growth modes of the helical chain in PLLA thin film can be modulated by the crystallization temperature. It is expected that our in situ study with local technique will provide some new insight on understanding the nature of crystallization temperature induced lamellar orientation in polymer thin film.

**Received:** April 4, 2011

**Revised:** July 31, 2011

**Published:** September 14, 2011

## 2. EXPERIMENTAL SECTION

**2.1. Material and Sample Preparation.** PLLA pellets, (Nature Works 2002D,  $M_w = 3.8 \times 10^5 \text{ g mol}^{-1}$ ,  $M_w/M_n = 1.6$ ) were dissolved in chloroform to prepare solution with concentration of 7.5 mg/mL. PLLA thin films were prepared on the gold-coated glass wafers (Au Substrates) by spin-coating method at a speed of 4000 rpm for 60s. Then the thin films were kept under vacuum pressure 0.1 kPa at 25 °C for 24 h to remove the residual solvent. The vacuum drying oven is made by Shanghai Boxun Industry and Commerce Co., Ltd. DZF-6020.

Au substrates were prepared by evaporating chromium (20 Å) and gold (800 Å) in sequence onto glass wafers with the size of 1.5 cm  $\times$  4 cm at rates of 1–2 Å s<sup>-1</sup> in a diffusion-pumped chamber with a base pressure of  $4 \times 10^{-6}$  Torr. Before using, the gold substrates were successively cleaned with deionized water, concentrated sulfuric acid-hydrogen peroxide solution (concentrated sulfuric acid/hydrogen peroxide water = 2:1), deionized water, pure ethanol, and dried in a stream of nitrogen.)

**2.2. Reflection–Absorption Infrared (RAIR) Measurement.** Reflection–absorption Infrared (RAIR) spectra were measured by a Bruker Tensor 27 spectrometer equipped with a MCT detector. To monitor the isothermal crystallization dynamics of PLLA thin film, a homemade heating stage was set into the accessory of RAIR. After the setting temperature of the heating stage is reached and turns to be stable, we first collect the background of Au substrate without sample and then put the sample on the heating stage and start to collect the RAIR spectra of the PLLA thin film during the annealing process. The measurements were obtained by averaging 32 scans and a resolution of 4 cm<sup>-1</sup>. The incidence angle is equal to 84° for obtaining the optimized signal/noise ratio and the polarization of the incoming beam was parallel to the plane of incidence.

**2.3. Polarized FTIR Spectra Measurement.** The PLLA films were obtained by casting solution in Petri dishes at room temperature. After the majority of the solvent had evaporated, the films were placed under vacuum at room temperature for 24 h to completely remove the residual solvent. Dynamic mechanical thermal analysis instrument (DMA) (Germany Gabo Company, Eplexor 500N) was used to slowly stretch the PLLA films at 65 °C with drawing ratio equal to 2. We choose the temperature at 65 °C because the temperature is a little higher than the glass transition temperature of PLLA (about 58 °C), and the crystallization rate is very slowly at this temperature. The spectra of PLLA film before and after stretching were measured by polarized FT-IR.

**2.4. Thickness Determination and Surface Morphology.** Atomic force microscope (AFM) (Agilent Technologies Company, Agilent-5500) was used to capture both the height and phase images at room temperature. First, the sample on the Au substrate was scratched with a needle. Then, the thicknesses of gold films and PLLA-gold films were measured by the height profiles of AFM, respectively. Finally, the thickness of PLLA thin films were acquired by subtracting the gold films thickness from that of PLLA-gold films. In the present work, the thickness of the PLLA thin films was  $\sim$ 80 nm.

## 3. RESULTS AND DISCUSSION

**3.1. Polarized IR Spectra of Uniaxially PLLA Film.** Before we discuss the orientation of PLLA chain in thin film with the RAIR data, it is necessary to summarize the characteristic bands of PLLA associated with the orientation effect. For this purpose, we

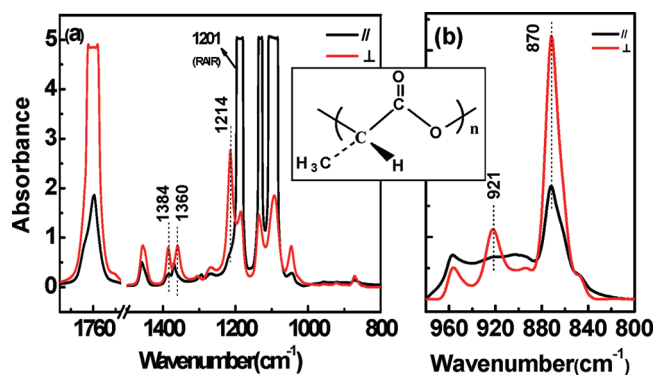


**Figure 1.** (a) Polarized IR spectra in the range 1820–800 cm<sup>-1</sup> of uniaxially oriented PLLA films. (b) Enlarged polarized IR spectra in the range 1000–800 cm<sup>-1</sup>.

measured the polarized IR spectra of uniaxially PLLA film. Usually, the polymer chain will be parallel to the drawing direction in uniaxially sample and the so-called parallel bands will be therefore enhanced when the polarized IR light is parallel to the drawing direction. In contrast, perpendicular bands will become stronger when perpendicular polarized IR light is used. As shown in Figure 1a, some of the perpendicular bands and parallel bands can be clearly identified. Because of the saturation of some bands, we get the peak position of parallel band around 1201 cm<sup>-1</sup> from the RAIR spectra, which will be shown later. Clearly, it is suggested that the band at 1360, 1214, 921, and 870 cm<sup>-1</sup> are the perpendicular bands, whereas the bands at 1370 and 1201 cm<sup>-1</sup> are the parallel ones. According to the molecular structure of PLLA as depicted in the inset graph of the figure, it is rational to figure out that the C=O stretching vibration region is located in the spectral region of 1860–1660 cm<sup>-1</sup>, whereas the spectral region of 1500–1000 cm<sup>-1</sup> is involved in the CH<sub>3</sub>, CH bending, and C–O–C stretching vibration.

Figure 1b shows the enlarged spectral region in the range of 970–800 cm<sup>-1</sup>, which is related to the backbone vibration of PLLA.<sup>39</sup> The bands at 920 cm<sup>-1</sup> is assigned to the coupling of C–C backbone stretching with the CH<sub>3</sub> rocking mode and it is sensitive to the 10/3 helix chain conformation of PLLA  $\alpha/\alpha'$  crystals,<sup>26</sup> whereas the band at 956 cm<sup>-1</sup> is associated with the amorphous phase of PLLA.<sup>15,18</sup> According to the references<sup>39,40</sup> and the polarized IR spectra presented here, the bands assignments of PLLA were summarized in Table 1.

**3.1. Microstructure and Morphology of PLLA Thin Films Cold Crystallized at Different Temperature.** The p-polarized RAIR spectra of PLLA thin films crystallized at 70, 80, 90, and 100 °C in the range of 1820–800 cm<sup>-1</sup> are shown in Figure 2a, Figure 2b shows the enlarged spectral region in the range of 980–845 cm<sup>-1</sup>. As shown in Figure 1b, for PLLA thin film crystallized at low temperature (70 and 80 °C), both the helical sensitive band at 921 cm<sup>-1</sup> and the crystalline band at 870 cm<sup>-1</sup> can be clearly identified. However, for the samples crystallized at higher temperature (90 and 100 °C), both of these two bands are very weak. The weak intensity of the amorphous band at 955 cm<sup>-1</sup> should be caused by the higher crystallinity for the samples crystallized at higher temperature. Considering that only the vibrations with the transition moment perpendicular to the gold substrate will be enhanced in p-polarized RAIR spectra, the weaker intensities of the crystalline sensitive bands at 921 and 870 cm<sup>-1</sup> should be caused by the orientation effect.

As shown in the enlarged spectra in Figure 3, obvious spectral difference can also be observed in the  $\text{CH}_3$  deformation vibration region and  $\text{C}-\text{O}-\text{C}$  stretching, which are located in the spectral region of  $1480-1320$  and  $1290-1060\text{ cm}^{-1}$ , respectively. First, the band at  $1360\text{ cm}^{-1}$  is dominated for the PLLA thin film crystallized at lower temperature ( $70$  and  $80^\circ\text{C}$ ). However, for samples crystallized at higher temperature ( $90$  and  $100^\circ\text{C}$ ), the

**Table 1. Infrared Bands Characteristic and Assignments of PLLA**

wavenumber/ $\text{cm}^{-1}$	polarization	assignments <sup>a</sup>
$1384\text{ cm}^{-1}$	$\perp$	$\delta_s(\text{CH}_3)$
$1370\text{ cm}^{-1}$	$//$	$\delta_s(\text{CH}_3) + \delta_1(\text{CH})$
$1360\text{ cm}^{-1}$	$\perp$	$\delta_s(\text{CH}_3) + \delta_1(\text{CH})$
$1214\text{ cm}^{-1}$	$\perp$	$r_{as}(\text{CH}_3) + \nu_{as}(\text{COC})$
$1188\text{ cm}^{-1}$	$//$	$r_{as}(\text{CH}_3) + \nu_{as}(\text{COC})$
$920\text{ cm}^{-1}$	$\perp$	$r(\text{CH}_3) + \nu(\text{C}-\text{C})$
$870\text{ cm}^{-1}$	$\perp$	$\nu(\text{C}-\text{COO})$

<sup>a</sup>.  $\delta$  = deformation vibration;  $r$  = in-plane rocking vibration;  $\nu$  = stretching vibration;  $s$  = symmetric;  $as$  = asymmetric.

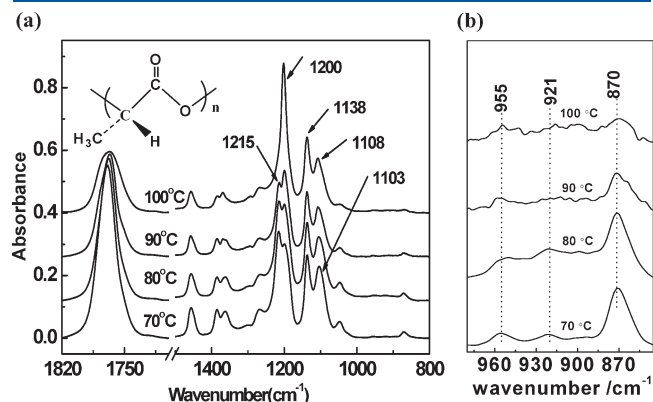


**Figure 2.** RAIR spectra in the range of  $1820-800\text{ cm}^{-1}$  (a) and the enlarged spectra in the range of  $980-845\text{ cm}^{-1}$  (b) for PLLA thin films crystallized at  $70$ ,  $80$ ,  $90$ , and  $100^\circ\text{C}$ .

intensity of band at  $1370\text{ cm}^{-1}$  is stronger. In a similar way, the bands at  $1214$  and  $1201\text{ cm}^{-1}$  are dominated for the sample crystallized at lower and higher temperature respectively.

As mentioned above, it is found that all the bands related with perpendicular orientation at  $1384$ ,  $1360$ ,  $1214$ ,  $921$ , and  $870\text{ cm}^{-1}$  are relatively enhanced in the spectra of PLLA thin film crystallized at lower temperature ( $70$  and  $80^\circ\text{C}$ ). In contrast, the bands in relation to parallel orientation at  $1370$  and  $1201\text{ cm}^{-1}$  are dominated for the samples crystallized at higher temperature ( $90$  and  $100^\circ\text{C}$ ). These observations strongly indicate that the molecular chains in these crystallized films demonstrate different orientations, which are dependent on the crystallization temperature.

According to the selection rule of p-polarized RAIR spectra, only the vibrations with the transition moment perpendicular to the metal surface will be detected as mentioned. Therefore, the relatively enhanced perpendicular bands in the RAIR spectra of PLLA thin films crystallized at lower temperature ( $70$  and  $80^\circ\text{C}$ ) indicate that the molecular chain is parallel to the gold substrate. As suggested by the appearance of the helical band at  $921\text{ cm}^{-1}$ , the molecular chain in the PLLA crystal takes the  $10/3$  helical conformation. It means that  $10/3$  helical chains are flat on the substrate for the PLLA thin films crystallized at lower temperature, whereas for the samples crystallized at higher temperature, their helical chains are perpendicular to the substrate.

It has been found that the crystallization temperature can affect the crystal modifications of PLLA. The ordered  $\alpha$  form and disordered  $\alpha'$  can be formed at high and low temperature, respectively. Both the  $\alpha$  and  $\alpha'$  form take the same  $10/3$  helical chains and there are mainly different in the chain packing modes. Therefore, the IR spectra of these two forms are highly similar. In our previous study,<sup>15</sup> it is found that the most notable spectral difference of these two forms is displayed in the  $\text{C}=\text{O}$  stretching region. For  $\alpha$  form of PLLA, obviously band splitting can be observed in the  $\text{C}=\text{O}$  stretching region. In the unpolarized spectra, three mainly bands at  $1776$ ,  $1759$ , and  $1749\text{ cm}^{-1}$  are discernible for  $\alpha$  form, whereas there are only two bands at  $1776$  and  $1760\text{ cm}^{-1}$  for  $\alpha'$  form.

The enlarged RAIR spectra and the second derivatives in the  $1820-1720\text{ cm}^{-1}$  range of PLLA thin films crystallized at various temperatures are shown in Figure 4. The intensity decrease of the bands in the  $\text{C}=\text{O}$  stretching region with increasing the

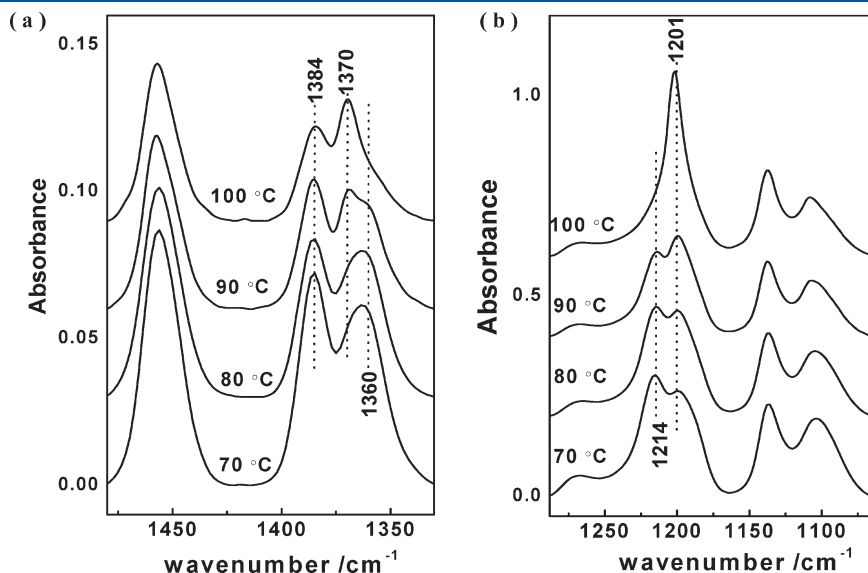


**Figure 3.** Enlarged RAIR spectra of PLLA thin films crystallized at  $70$ ,  $80$ ,  $90$ , and  $100^\circ\text{C}$  in the range of  $1480-1320\text{ cm}^{-1}$  (a) and  $1290-1060\text{ cm}^{-1}$  (b).



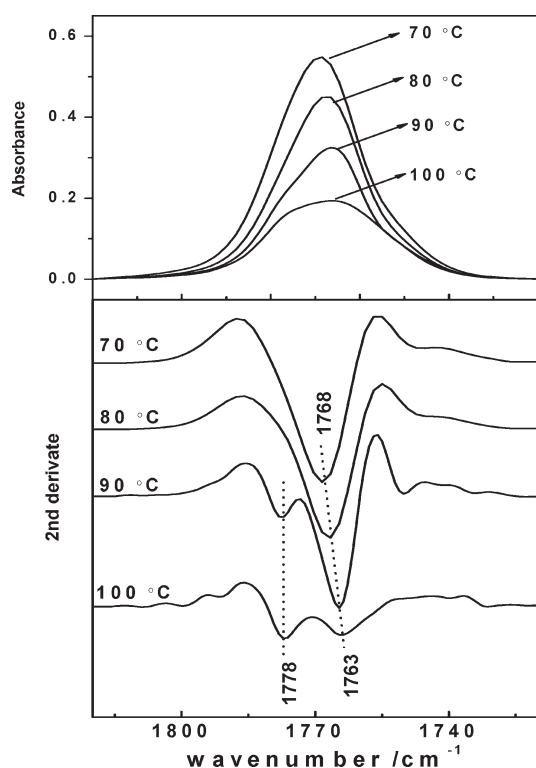


**Figure 4.** Enlarged RAIR spectra and the second derivatives in the 1820–1720  $\text{cm}^{-1}$  range of PLLA thin films crystallized at 70, 80, 90, and 100  $^{\circ}\text{C}$ .

crystallization temperatures should be related to the orientation change of the polymer chains. The shift of the bands at 1768 to 1763  $\text{cm}^{-1}$  may reflect that the crystal turns to more ordered with increasing the crystallization temperature. However, the characteristic band of PLLA  $\alpha$  at 1749  $\text{cm}^{-1}$  does not appear in all samples, it indicates that the helical chain packing in the crystal of these PLLA thin films is not as closing as that in the bulk sample of PLLA  $\alpha$  form.

For strengthening the conclusion on the chain orientation from the above spectral analysis, we observed the crystal morphologies of PLLA thin films crystallized at 70 and 100  $^{\circ}\text{C}$  by AFM. As shown in the height and phase images of Figure 5, there are preferentially edge-on and flat on lamellar crystals for the PLLA thin films crystallized at 70 and 100  $^{\circ}\text{C}$ , respectively. It is well-known that the polymer chain is folded into the lamellar and its direction is perpendicular to the folding surface. Moreover, the lamellar thickness of semicrystalline polymer is usually around 10 nm. Thus, the folding chain should be parallel to the substrate in the edge on lamellar, whereas it is perpendicular to the substrate for the flat on crystal. This conclusion is consistent with the above result derived from the RAIR data.

To illustrate the different molecular chain orientations, the schematic representation of the edge-on and flat-on lamellar crystal is shown in Figure 6. It should be mentioned that, the effect of crystallization temperature on the lamellar orientation is also observed in other polymer thin film, such as poly(ethylene oxide) and poly(bisphenol A hexane ether) etc.<sup>9,34,38</sup> For explaining the origin of such phenomena, Wang et al.<sup>38</sup> proposed that polymer chain mobility is strongly affected by the thickness of the films, temperature, and the interactions between the polymer and substrate. By dynamic Monte Carlo simulations of polymer crystallization confined in thin films, Ma et al.<sup>7</sup> found that the

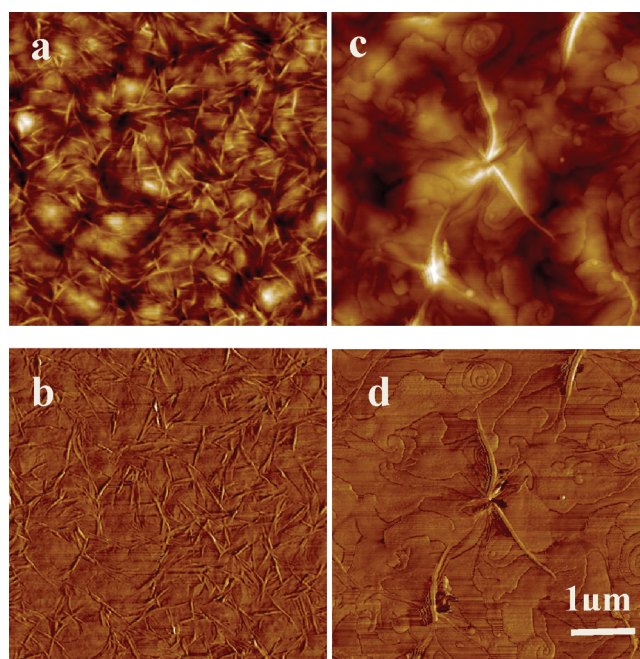


**Figure 5.** AFM images of PLLA thin film annealed at 70  $^{\circ}\text{C}$  (a, b) and 100  $^{\circ}\text{C}$  (c, d). Height (a, c) and phase (b, d) images are in the upper and lower rows, respectively.

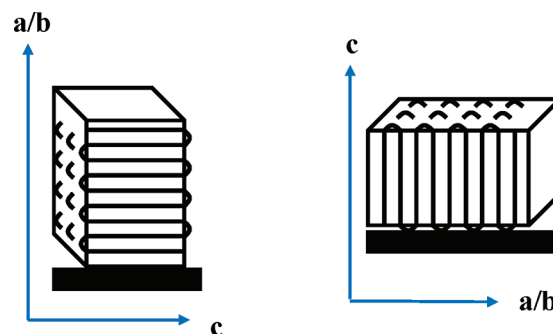


**Figure 6.** Schematic illustration of the edge-on (a) and flat-on (b) lamellar crystal of PLLA thin films.

surface-assisted crystal nucleation results in dominant edge-on lamellar crystals at high temperature; on the contrary, the random crystal nucleation yields preferentially flat-on lamellar crystals. However, the unambiguous conclusion has not been reached yet.

**3.2. Cold Crystallization Dynamics of PLLA Investigated by In Situ RAIR.** To examine the various orientation growth dynamics of PLLA, the in situ RAIR spectra were collected during the isothermal crystallization process PLLA thin films at 70 and 100  $^{\circ}\text{C}$ , respectively. (time interval 4 min) The spectral changes in the region of 1320–1000  $\text{cm}^{-1}$  are shown in Figure 7, in which the difference spectra obtained by subtraction of the initial spectrum are also displayed. With the increasing of annealing time, the intensities of the band at 1270  $\text{cm}^{-1}$  decrease for both the PLLA thin films crystallized at 70 and 100  $^{\circ}\text{C}$ . However, the perpendicular band at 1214 and 1200  $\text{cm}^{-1}$  and the parallel band at 1201  $\text{cm}^{-1}$  increase with time at 70 and 100  $^{\circ}\text{C}$ , respectively. Obviously, the band at 1270  $\text{cm}^{-1}$  should be associated with the amorphous phase of PLLA. The gradually increase of the bands at 1214 and 1200  $\text{cm}^{-1}$  in relation to the perpendicular

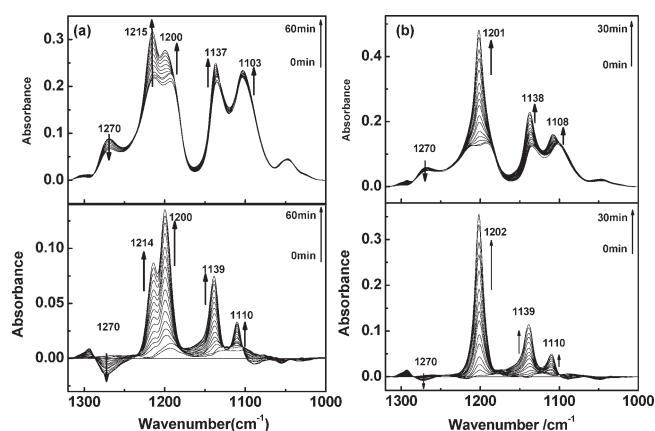


**Figure 7.** Temporal changes of the RAIR spectra and the corresponding difference spectra in the range of 1320–1000  $\text{cm}^{-1}$  collected every 1 min during the cold-crystallization process of PLLA thin film at (a) 70 °C (b) 100 °C, respectively.

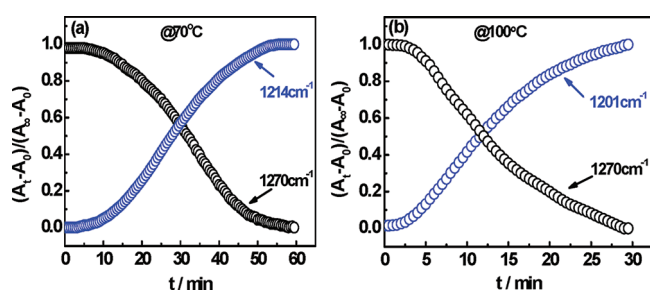


**Figure 8.** Intensity changes of the crystalline sensitive bands and amorphous bands of PLLA thin films as a function of crystallization time at (a) 70 and (b) 100 °C.

and parallel orientation respectively at 70 and 100 °C suggests that the orientation growths of PLLA chain at various temperature are started from the early stage of the cold crystallization.

For erasing the effect of film thickness on the band intensity in various samples, normalized peak intensities  $((A_t - A_0)/(A_\infty - A_0))$  of the crystalline sensitive bands at 1214  $\text{cm}^{-1}$  (70 °C), 1201  $\text{cm}^{-1}$  (100 °C) and the amorphous band at 1270  $\text{cm}^{-1}$  are plotted as a function of crystallization time in Figure 8.

To further understand the isothermal cold crystallization dynamics process of PLLA thin, the Avrami equation<sup>18,41,42</sup> was used, it can be stated as follows:

$$\frac{A_t - A_\infty}{A_0 - A_\infty} = \exp(-kt^n) \quad (1)$$

where  $A_t$  is the peak intensity at the crystallization time  $t$ ,  $A_0$  and  $A_\infty$  are, respectively, the initial and final peak intensities during isothermal cold crystallization,  $k$  is the crystallization rate constant,  $t$  is the time of the crystallization, and  $n$  is the Avrami exponent, which is related to the nature of nucleation and to the geometry of the growing crystals. Equation 1 can also be expressed in the form of the eq 2

$$\ln \left[ -\ln \left( \frac{A_t - A_\infty}{A_0 - A_\infty} \right) \right] = \ln k + n \ln t \quad (2)$$

By plotting the first term versus  $\ln t$ , the Avrami parameters  $n$  and  $k$  can be obtained from the slope and the intercept, respectively.

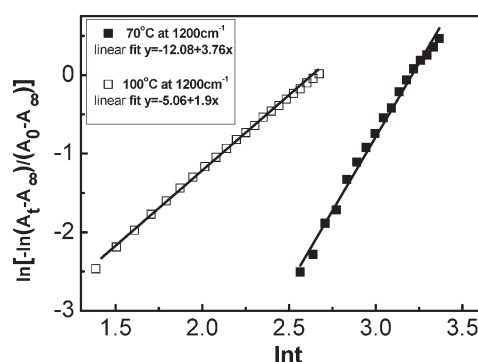


**Figure 9.** Example of the plot of Avrami equation for the isothermal cold crystallization of PLLA thin film at 70 and 100 °C. The peak height of the band at 1200  $\text{cm}^{-1}$  is used for this plot.

**Table 2.** Avrami Parameters Derived From the Analysis of Isothermal Cold Crystallization of PLLA at 70 and 100 °C

parameters (70 °C)	bands used for calculation ( $\text{cm}^{-1}$ )			
	1215	1200	1138	av
rate constant, $k(\text{min}^{-n} \times 10^5)$	1.63	1.02	1.67	1.44
Avrami index, $n$	3.41	3.59	3.42	3.47
half-time, $t_{1/2}(\text{min})$	23	22	22	22

parameters (100 °C)	bands used for calculation ( $\text{cm}^{-1}$ )			
	1215	1200	1138	av
rate constant, $k(\text{min}^{-n} \times 10^3)$	1.31	1.67	1.12	1.37
Avrami index, $n$	2.01	1.93	2.07	2.00
half-time, $t_{1/2}(\text{min})$	12	12	11	12

Figure 9 gives an example of the plot of Avrami equation the peak height of the band at 1200  $\text{cm}^{-1}$  for the isothermal cold crystallization of PLLA thin film at 70 and 100 °C.

The half-life  $t_{1/2}$  is an important parameter for the discussion of the crystallization kinetics and can be expressed as follows:

$$t_{1/2} = \left( \frac{\ln 2}{k} \right)^{1/n} \quad (3)$$

The parameters of crystallization kinetics calculated from several crystalline sensitive bands shown in the difference spectra of Figure 7 are listed in Table 2.

From Table 2, we can see that the average value of the Avrami exponent is  $n \approx 3.47$  for PLLA thin film crystallized at 70 °C, whereas it is  $n \approx 2$  for that crystallized at 100 °C. Usually, the Avrami exponent for semicrystalline polymers is thought to be associated with the crystal growth dimensional and nucleation modes.<sup>41,42</sup> For the system of heterogeneous nucleation, the crystal growth dimensional is equal to  $n$ , whereas it is equal to  $n-1$  for homogeneous nucleation mode.<sup>18</sup> For PLLA thin film crystallized at 70 °C, Avrami exponent ( $n \approx 3.47$ ) suggests that the crystallization start from homogeneous nucleation and the crystal growth corresponds to either 2-D ( $n = 3$ ) or 3-D ( $n = 4$ ) crystallization. While we find the different phenomenon at 100 °C, the Avrami exponent is  $n \approx 2$ , which suggest that crystallization start from heterogeneous nucleation and the crystal growth correspond to two-dimensional. Obviously, annealing temperature

has great influence on nucleation and crystal growth. With the increase of annealing temperature, the nucleation mode changes from homogeneous nucleation to heterogeneous nucleation, this is consistent with some report in the literature.<sup>8,35</sup>

#### 4. CONCLUSIONS

In the present work, the effect of crystallization temperature on the molecular chain orientation and the crystallization dynamics of PLLA thin film are investigated by in situ RAIR techniques. It is found that, in the temperature range from 70 to 100 °C, the helical chains in the PLLA film are parallel to the substrate at low temperature, whereas they are perpendicular to the substrate at high temperature. Such conclusion is consistent with the observation from AFM images, that is, edge-on and flat-on lamellar crystals of PLLA are formed at low and high temperature, respectively. Clearly, it is found that the orientation of helical chain and lamellar in PLLA thin film can be modulated by the crystallization temperature. Moreover, it is found that the orientation of helical chain is started from the early stage of the isothermal crystallization process and such orientation can be kept during the whole crystallization process. Finally, the analysis on the crystallization dynamics of PLLA thin film demonstrates that the crystal growth dimensional and nucleation modes are also strongly affected by the crystallization temperature.

#### AUTHOR INFORMATION

##### Corresponding Author

\*Tel: +86-532-84022604. Fax: +86-532-84022791. E-mail: zjm@qust.edu.cn.

#### ACKNOWLEDGMENT

The financial supports from Natural Science Foundation of China (20804004), Shandong Province Science Foundation for Distinguished Young Scholars (JQ200905), Taishan Mountain Scholar Constructive Engineering Foundation (TS20081120) and Doctoral Fund of Qingdao University of Science and Technology are greatly appreciated.

#### REFERENCES

- (1) Kong, X. M.; He, S. G.; Wang, K. H.; Xie, X. M. *Spectrosc. Spectral Anal.* **2004**, *17*, 806.
- (2) Wang, Z.; Xie, X. M.; Yang, R.; Wang, X. F. *Chem. J. Chinese Univ.* **2006**, *27*, 161.
- (3) Kong, X. M.; He, S. G.; Wang, Z.; Chen, Z.; Xie, X. M. *Acta Polym. Sin.* **2003**, *4*, 571.
- (4) Zhang, Y.; Zhang, J. M.; Lu, Y. L.; Duan, Y. X.; Yan, S. K.; Shen, D. Y. *Macromolecules* **2004**, *37*, 2532.
- (5) Schonherr, H.; Frank, C. W. *Macromolecules* **2003**, *36*, 1188.
- (6) Schonherr, H.; Frank, C. W. *Macromolecules* **2003**, *36*, 1199.
- (7) Ma, Y.; Hu, W.; Reiter, G. *Macromolecules* **2006**, *39*, 5159.
- (8) Wang, Y.; Chan, C. M.; Ng, K. M.; Li, L. *Macromolecules* **2008**, *41*, 2548.
- (9) Wang, Y.; Ge, S.; Rafailovich, M.; Sokolov, J.; Zou, Y.; Ade, H.; Luning, J.; Lustig, A.; Maron, G. *Macromolecules* **2004**, *37*, 3319.
- (10) Mareau, V. H.; Prudhomme, R. E. *Macromolecules* **2005**, *38*, 398.
- (11) Ye, S.; Morita, S.; Li, G. F.; Noda, H.; Tanaka, M.; Uosaki, K.; Osawa, M. *Macromolecules* **2003**, *36*, 5694.
- (12) Elzein, T.; Brogly, M.; Schultz, J. *Polymer* **2002**, *43*, 4811.
- (13) Lorenzo, M. L. D. *Eur. Polym. J.* **2005**, *41*, 569.
- (14) Zhang, J. M.; Tashiro, K.; Tsuji, H.; Domb, A. J. *Macromolecules* **2007**, *40*, 1049.
- (15) Zhang, J. M.; Duan, Y. X.; Sato, H.; Tsuji, H.; Noda, I.; Yan, S. K.; Ozaki, Y. *Macromolecules* **2005**, *38*, 8012.
- (16) Abe, H.; Kikkawa, Y.; Inoue, Y.; Doi, Y. *Biomacromolecules* **2004**, *5*, 1606.
- (17) Ikada, Y.; Tsuji, H. *Macromol. Rapid Commun.* **2000**, *21*, 117.
- (18) Zhang, J. M.; Tsuji, H.; Noda, I.; Ozaki, Y. *Macromolecules* **2004**, *37*, 6433.
- (19) Krikorian, V.; Pochan, D. J. *Macromolecules* **2005**, *38*, 6520.
- (20) Rahman, N.; Kawai, T.; Matsuba, G.; Nishida, K.; Kanaya, T.; Watanabe, H.; Okamoto, H.; Kato, M.; Usuki, A.; Matsuda, M.; Nakajima, K.; Honma, N. *Macromolecules* **2009**, *42*, 4739.
- (21) Cartier, L.; Okihara, T.; Ikada, Y.; Tsuji, H.; Puiggali, J.; Lotz, B. *Polymer* **2000**, *41*, 8909.
- (22) Pan, P. J.; Inoue, Y. *Prog. Polym. Sci.* **2009**, *34*, 605.
- (23) Alemán, C.; Lotz, B.; Puiggali, J. *Macromolecules* **2001**, *34*, 4795.
- (24) Yuryev, Y.; Adams, P. W.; Heuzey, M. C.; Dubois, C.; Brisson, J. *Polymer* **2008**, *49*, 2306.
- (25) Zhang, J. M.; Tsuji, H.; Noda, I.; Ozaki, Y. *J. Phys. Chem. B* **2004**, *108*, 11514.
- (26) Zhang, J. M.; Tashiro, K.; Tsuji, H.; Domb, A. J. *Macromolecules* **2008**, *41*, 1352.
- (27) Damien, M.; Robert, E. *Macromolecules* **2008**, *41*, 1705.
- (28) Chen, D. J.; Gong, Y. M.; He, T. B.; Zhang, F. J. *Macromolecules* **2006**, *39*, 4101.
- (29) Ho, R. M.; Hsieh, P. Y.; Tseng, W. H.; Lin, C. C.; Huang, B. H.; Lotz, B. *Macromolecules* **2003**, *36*, 9085.
- (30) Zhang, J. M.; Zhang, D. H.; Shen, D. Y. *Macromolecules* **2002**, *35*, 5140.
- (31) Elzein, T.; Brogly, M.; Castelein, G.; Schultz, J. *Polymer* **2002**, *40*, 1464.
- (32) Mate, B.; Ortega, I. K.; Moreno, M. A.; Herrero, V. J.; Escrivano, R. *J. Phys. Chem. B* **2006**, *110*, 7396.
- (33) Subramanian, S.; Sampath, S. *Biomacromolecules* **2007**, *8*, 2120.
- (34) Zhang, Y.; Mukoyama, S.; Hu, Y.; Yan, C.; Ozaki, Y.; Takahashi, I. *Macromolecules* **2007**, *40*, 4009.
- (35) Piwowar, A. M.; J. A., G., Jr. *Macromolecules* **2008**, *41*, 2616.
- (36) Liang, Y. R.; Zheng, M. Z.; Park, K. H.; Lee, H. S. *Polymer* **2008**, *49*, 1961.
- (37) Dong, H. L.; Li, H. X.; Wang, E. J.; Yan, S. K.; Zhang, J. M.; Yang, C. M.; Takahashi, I.; Nakashima, H.; Torimitsu, K.; Hu, W. P. *J. Phys. Chem. B* **2009**, *113*, 4176.
- (38) Wang, Y.; Chan, C. M.; Ng, K. M.; Li, L. *Macromolecules* **2008**, *41*, 2548–2553.
- (39) Kister, G.; Cassanas, G.; Vert, M. *Polymer* **1998**, *39*, 267.
- (40) Kang, S.; Hsu, S. L.; Stidham, H. D.; Smith, P. B.; Leugers, M. A.; Yang, X. *Macromolecules* **2001**, *34*, 4542.
- (41) Avrami, M. *J. Chem. Phys.* **1939**, *7*, 1103.
- (42) Avrami, M. *J. Chem. Phys.* **1940**, *8*, 212.